

See discussions, stats, and author profiles for this publication at: <https://www.researchgate.net/publication/256490773>

Dissociation of Antimicrobial and Hemolytic Activities of Gramicidin S through N-Methylation Modification

ARTICLE *in* CHEMMEDCHEM · NOVEMBER 2013

Impact Factor: 2.97 · DOI: 10.1002/cmdc.201300232 · Source: PubMed

READS

50

8 AUTHORS, INCLUDING:



Yangmei Li

Torrey Pines Institute for Molecular Studies

16 PUBLICATIONS 124 CITATIONS

SEE PROFILE



Nina Bionda

iFyber

19 PUBLICATIONS 88 CITATIONS

SEE PROFILE



Predrag Cudic

Torrey Pines Institute for Molecular Studies

44 PUBLICATIONS 578 CITATIONS

SEE PROFILE



Richard Houghten

Torrey Pines Institute for Molecular Studies

554 PUBLICATIONS 23,550 CITATIONS

SEE PROFILE

Dissociation of Antimicrobial and Hemolytic Activities of Gramicidin S through N-Methylation Modification

Yangmei Li,* Nina Bionda, Austin Yongye, Phaedra Geer, Maciej Stawikowski, Predrag Cudic, Karina Martinez, and Richard A. Houghten*[a]

β -Sheet antimicrobial peptides (AMPs) are well recognized as promising candidates for the treatment of multidrug-resistant bacterial infections. To dissociate antimicrobial activity and hemolytic effect of β -sheet AMPs, we hypothesize that N-methylation of the intramolecular hydrogen bond(s)-forming amides could improve their specificities for microbial cells over human erythrocytes. We utilized a model β -sheet antimicrobial peptide, gramicidin S (GS), to study the N-methylation effects on the antimicrobial and hemolytic activities. We synthesized twelve N-methylated GS analogues by replacement of residues at the β -strand and β -turn regions with N-methyl amino acids, and tested their antimicrobial and hemolytic activities. Our experiments showed that the HC_{50} values increased fivefold compared with that of GS, when the internal hydrogen-bonded

leucine residue was methylated. Neither hemolytic effect nor antimicrobial activity changed when proline alone was replaced with N-methylalanine in the β -turn region. However, analogues containing N-methylleucine at β -strand and N-methylalanine at β -turn regions exhibited a fourfold increase in selectivity index compared to GS. We also examined the conformation of these N-methylated GS analogues using 1H NMR and circular dichroism (CD) spectroscopy in aqueous solution, and visualized the backbone structures and residue orientations using molecular dynamics simulations. The results show that N-methylation of the internal hydrogen bond-forming amide affected the conformation, backbone shape, and side chain orientation of GS.

Introduction

The emergence of multidrug-resistant bacteria has led to an urgent need for the development of new antibiotics. β -Sheet antimicrobial peptides (AMPs), for example, tachyplesin,^[1] protegrin-1,^[2] arenicin,^[3] lactoferricin B,^[4] Ib-AMP1,^[5] gomesin,^[6] and RTD-1,^[7] are a class of host defense peptides that potently inhibit the growth of Gram-positive and Gram-negative pathogens. These peptides present key structural elements for antiparallel β -sheet strand and amphiphilic character for biological activity. The mechanism of action of β -sheet AMPs is generally accepted as the disruption of the bacterial cell membrane through a detergent-like behavior. Resistance is less likely to develop when this mechanism is involved since it requires significant changes of bacterial membrane composition. Beside the disruption of membranes, many β -sheet AMPs were also found that inhibited intracellular targets.^[8] Thus, β -sheet AMPs are well recognized as promising candidates for developing novel antibiotics for the treatment of multidrug-resistant bacteria infections.


Degradation and toxicity are two major hurdles in developing β -sheet AMPs for therapeutic use. Generally, degradation

of peptide is caused by proteolysis in vivo and can be substantially decreased by introduction of D-amino acids, cyclization, and other chemical manipulation modifications. Toxicity of β -sheet AMPs is usually associated with hemolysis, which is the result of strong amphiphilic structure of these peptides. Therefore, tuning amphiphilicity to improve their selectivity for bacterial cells over human erythrocytes plays a key role in the development of β -sheet AMPs for therapeutic use, in particular systemic use.

Intramolecular hydrogen bonds between an antiparallel β -strand stabilize the conformation of β -sheet AMPs and amphiphilicity thereof. Methylation of internal hydrogen-bonded amides in the antiparallel β -strand disrupts the intramolecular hydrogen bond(s) and reduces the structural order (Figure 1 a). We hypothesize that disruption of the intramolecular hydrogen bond(s) may perturb amphiphilicity of β -sheet AMPs, therefore improving selectivity between microbial and host cells. To illustrate how N-methylation impacts biological activity of β -sheet AMPs, we utilized gramicidin S (GS) as a model β -sheet AMP to test this hypothesis. GS is a typical cyclic β -sheet AMP, which has the antiparallel β -sheet strand stabilized by two β -hairpin motifs made up of D-Phe-Pro. Two cationic Orn residues are on one side of the molecule and four hydrophobic Leu and Val residues are on the opposite side (Figure 1 b). Thus GS serves as an excellent model for studying β -sheet antimicrobial peptides.

GS is currently limited to topical application due to lack of selectivity required for a human antibiotic for systemic use. To

[a] Dr. Y. Li, Dr. N. Bionda, Dr. A. Yongye, P. Geer, Dr. M. Stawikowski, Dr. P. Cudic, Dr. K. Martinez, Dr. R. A. Houghten
Torrey Pines Institute for Molecular Studies
11350 SW Village Parkway, Port Saint Lucie, FL 34987 (USA)
E-mail: yli@tpims.org
Houghten@tpims.org

 Supporting information for this article is available on the WWW under <http://dx.doi.org/10.1002/cmdc.201300232>.

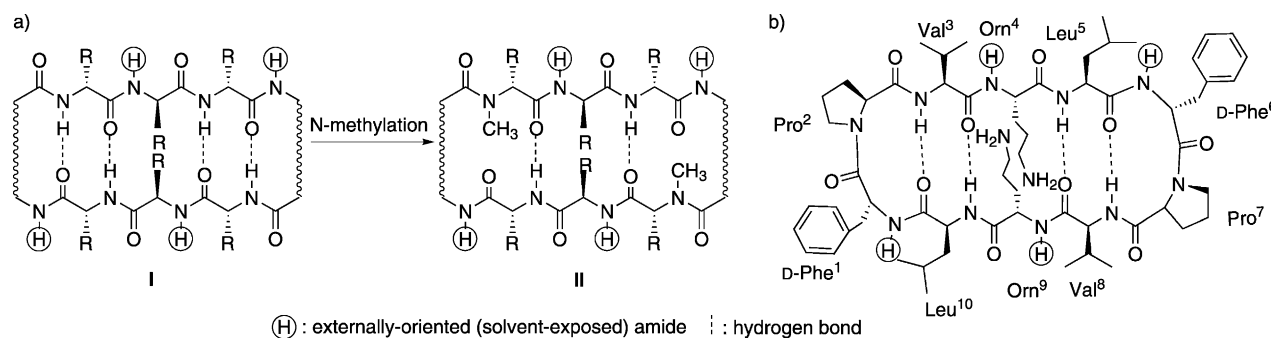


Figure 1. a) The β -Sheet conformation of antimicrobial peptides (I) and hydrogen-bond disruption by N-methylation (II). b) Structure of GS.

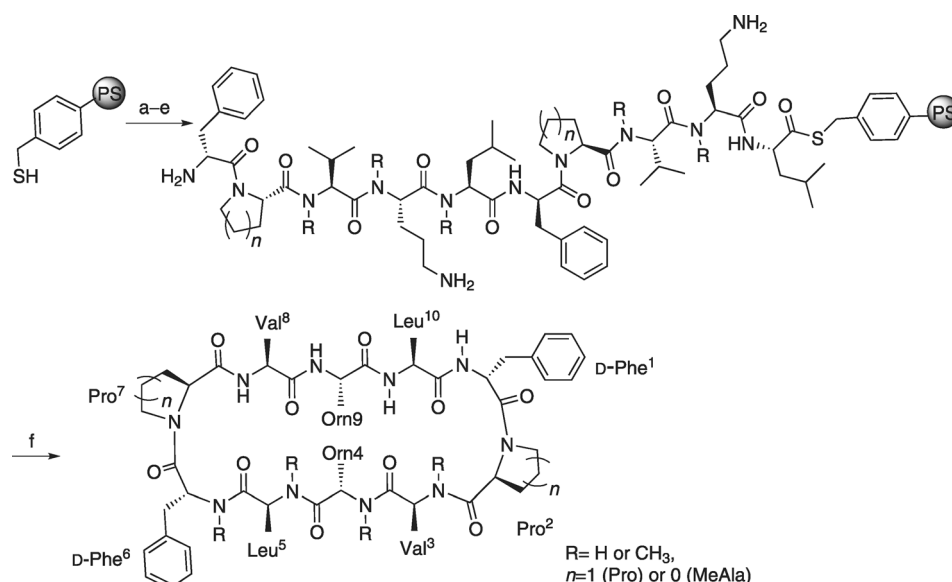
dissociate the antimicrobial activity from the hemolytic activity of GS, structural modifications, in particular on the β -hairpin and the ring size, have been carried out to improve the selectivity.^[9] Replacing D-Phe residues at the turn regions with surrogates have been reported to strongly modulate the therapeutic index of GS.^[10] A series of ring-expanded analogues having 12-, 14-, and 16-peptidyl residues have been synthesized. Their conformation, amphiphilicity, and self-association propensity have been investigated in detail.^[11] Although many studies have been done to improve the selectivity of GS, the effects of N-methylation of amides, particularly different types of amides, on biological activities and backbone conformations have not yet been known.

In this study, we synthesized GS analogues in which N-methylated amino acids were used at β -strand region to replace residues whose amide protons are known to be either involved in internal hydrogen bonds or are exposed externally. Since Pro delivers a strong effect on conformation, dominates at β -turn region in proteins and peptides, and shows structural similarity to N-methyl-L-alanine (MeAla),^[12] we also replaced the Pro at β -turn regions with MeAla. We tested the antimicrobial activity and the hemolytic effect for these N-methylated GS (NMe-GS) analogues. We examined their conformation using ¹H NMR and circular dichroism (CD) spectroscopy in aqueous solution, and visualized the backbone structure and residue orientation through molecular dynamics simulations. Herein, we present the results from the biological investigation as well as the conformational studies of these NMe-GS analogues.

Results and Discussion

Synthesis

To investigate the effects of N-methylation at specific sites on the biological activity of GS, we designed 12 N-methylated GS (NMe-GS) analogues. The sequences of each analogue are shown in Scheme 1. Six out of twelve analogues were monomethylated (NMe-1 to -6), including four compounds (NMe-1 to -4) each consisting of a single amino acid substituted with a N-methyl-L-alanine (MeAla)—a MeAla scan, one compound (NMe-5) containing a Leu substituted with an N-methyl-L-leucine (MeLeu), and one compound (NMe-6) having a D-Phe substituted with an N-methyl-D-phenylalanine (MeD-Phe). Four analogues (NMe-7 to -10) were dimethylated, each compound containing one Pro replaced with a MeAla and a second amino acid replaced with an N-methylated amino acid. Two analogues were trimethylated (NMe-11 to -12), each having one Pro substituted with a MeAla and two other amino acids substituted with N-methylated amino acids.



Scheme 1. Synthesis of GS and the N-methylated analogues. *Reagents and conditions:* a) Boc-Leu-OH/PyBOP/DIEA (5:5:7.5 equiv), overnight; b) TFA/CH₂Cl₂ (55% v/v), 30 min, then DIEA/CH₂Cl₂ (5% v/v); c) Boc-Orn(Z)-OH/DIC/HOBt (5:5:5 equiv), 2 h; d) TFA/CH₂Cl₂ (55% v/v), 30 min, then DIEA/CH₂Cl₂ (5% v/v); e) repeat step c) and d) to complete resin-bound linear peptides; f) anhyd HF, 0 °C, 2 h; g) DIEA/DMF (10% v/v), overnight.

Table 1. Antimicrobial and hemolytic activity of GS and N-methylated analogues.

Compd	MIC ₉₀ [μM] ^[a]						HC ₅₀ [μM] ^[b]	Type of amide methylated	Residue alternation	t _R [min] ^[c]
	Gram (+) pathogens ^[d]			Gram (−) pathogens ^[e]						
	MDRSA	VRSA	MRSE	<i>E. coli</i>	<i>K. pne.</i>	<i>Salm.</i>				
GS	1.8	3.6	1.8	28	3.6	28	14.3 ± 1.45	–	–	4.557
NMe-1	56	56	28	56	56	> 56	> 56 ^[f]	internal	MeAla ⁵	4.124
NMe-2	3.1	12.6	3.1	> 50.4	3.6	> 50.4	17.1 ± 0.5	external	MeAla ⁴	5.637
NMe-3	> 37 ^[g]	> 37	18.6	> 37	> 37	> 37	39.0 ± 3.0	internal	MeAla ³	3.709
NMe-4	3.6	3.6	1.8	28	3.6	29	14.2 ± 0.75	Pro	MeAla ²	4.512
NMe-5	8.7	8.7	1.7	34.6	8.7	34.6	75.4 ± 0.63	internal	MeLeu ⁵	4.420
NMe-6	2.6	10.4	1.7	45	5.2	22.5	13.0 ± 1.0	external	MePhe ⁶	4.589
NMe-7	58	116	14.5	116	116	116	> 116	internal	MeAla ² , MeAla ⁵	4.110
NMe-8	7	3.5	1.8	28	7	28	69.2 ± 1.3	internal	MeLeu ⁵ , MeAla ⁷	4.482
NMe-9	3.5	6.1	0.4	48	3.5	24.5	14.4 ± 0.65	external	MeAla ² , Mephe ⁶	4.594
NMe-10	1.8	3.6	0.9	30.4	3.6	30.4	16.3 ± 2.1	Pro, Pro	MeAla ² , MeAla ⁷	4.514
NMe-11	7.1	7.1	3.5	56.6	14.2	56.6	94.1 ± 9.9	Internal, Pro	MeAla², MeLeu⁵, MeAla⁷	4.453
NMe-12	114.8	114.8	57.4	57.4	114.8	> 114.8	> 114.8	Internal, Pro	MeAla ² , MeAla ⁵ , Mephe ⁶	4.129

[a] MIC₉₀: minimum inhibitory concentration that inhibits 90% of bacterial isolates after 20 h, relative to a control culture. Data are the representative values of two duplicate experiments performed in duplicate, and the experimental error is one MIC interval. [b] HC₅₀: 50% hemolytic concentration is the minimum concentration required for lysis 50% of human erythrocytes. Data represent the mean of representative values of two duplicate experiments performed in triplicate ± SD. [c] Retention time (t_R) is determined by reversed-phase HPLC; column: Luna 5μ C18, 50 × 4.6 mm; method: linear gradient 5 → 95% solvent B (0.1% formic acid in CH₃CN) over 6 min; solvent A (0.1% formic acid in H₂O). [d] Gram-positive pathogens included multidrug-resistant *S. aureus* ATCC-BAA-44 (MDRSA), vancomycin-resistant *S. aureus* (VRSA), methicillin-resistant *S. epidermidis* (VRSE). [e] Gram-negative pathogens included *E. coli* k-12 (*E. coli*), *K. pneumonia* (*K. pne.*), *Salmonella* (*Salm.*). [f] Sample concentrations ranging from 62 to 0.5 μg mL^{−1}, exhibited 4.3% hemolysis at 56 μg (62 μg mL^{−1}). [g] Sample concentrations ranging from 42 to 0.3 μg mL^{−1}.

We synthesized GS and NMe-GS analogues using a solid-phase synthetic approach as shown in Scheme 1. Polystyrene-based mercaptomethylphenyl resin was used as support for the synthesis. The *tert*-butoxycarbonyl (Boc)-protected amino acid was coupled stepwise on the resin to form the resin-bound decapeptide thioester. Because thioesters are resistant to hydrogen fluoride (HF), the protecting groups of the resin-bound peptide thioesters were removed with anhydrous HF.^[13] The desired cyclic peptides were then released through cyclization/cleavage by the treatment of the resin bound peptide thioesters with *N,N*-diisopropylethylamine (DIEA; 10% v/v in *N,N*-dimethylformamide, DMF). GS synthesized using this method exhibited identical molecular weight and HPLC retention time to a standard GS sample (Sigma–Aldrich), indicating the synthetic GS is exactly same as the standard one.

Antimicrobial activity

The antimicrobial activities of the synthetic GS and the NMe-GS analogues were tested against a variety of multidrug-resistant Gram-positive and Gram-negative bacteria using a standard microdilution broth assay.^[14] Bacterial strains included multidrug-resistant *Staphylococcus aureus* (MDRSA) BAA-44, vancomycin-resistant *S. aureus* (VRSA), methicillin-resistant *S. epidermidis* (MRSE), *Escherichia coli*, *Klebsiella pneumoniae*, and *Salmonella*. Minimum inhibitory concentration (MIC₉₀) of each compound against each strain was determined (Table 1). Substitution with N-methylated amino acid at varying sites affected the antimicrobial activity differently. Compared to GS, the average MIC₉₀ value against Gram-positive bacteria increased 15–20-fold when one internal hydrogen bond-forming residue, Leu or Val, was replaced with MeAla (NMe-1 and NMe-3), but

remained almost unchanged when Leu was replaced with MeLeu (NMe-5). This result suggests that Leu may be essential for the antimicrobial activity. The antimicrobial activity was also not affected when a single externally exposed residue, Orn or D-Phe, was replaced with N-methylated amino acids (NMe-2 and NMe-6). Since NMe-2 has a Orn⁴ → MeAla⁴ replacement, which is not a conservative replacement, this unaffected antimicrobial activity could possibly be explained by two effects: methylation of the externally exposed amide did not affect the antimicrobial activity, or only one positively charged Orn was essential for keeping the antimicrobial activity. Replacement of Pro with MeAla (NMe-4 and NMe-10) did not change the antimicrobial activity as compared to GS as well.

Hemolytic activity

The hemolytic activity for each compound was also examined. The minimal concentration of each compound required for 50% lysis of human red blood cells (HC₅₀) was determined (Table 1). The HC₅₀ value of the synthetic GS, 16 μg mL^{−1}, is identical to the standard GS in our experiment, and is similar to that reported.^[15] As seen from the HC₅₀ values, N-methylated amino acid substitutions exhibited site-specific effects on the hemolytic activity as well. Substitution of the internal hydrogen bond-forming residues with N-methylated amino acids, either MeAla or the matching N-methylated amino acid, increased HC₅₀ values up to fivefold compared to that of GS, indicating the hemolytic effects of those NMe-GS analogues decreased. Substitution of the residues having externally exposed amide protons with N-methylated amino acids did not affect the HC₅₀. The HC₅₀ value remained unchanged when Pro was the only residue that was replaced by MeAla, no matter if one

or both Pro were replaced (NMe-4 and NMe-10), but remarkably increased when an internal hydrogen bond-forming residue was also methylated (NMe-7, NMe-8, and NMe-11), suggesting that N-methylation of internal hydrogen bond-forming residues is responsible for the decrease of the hemolytic activity.

N-Methylated amino acid substitutions at different positions on GS exhibited varying effects on the selectivity and specificity. Selectivity indices (SI), designated as the ratio of HC_{50} to MIC_{90} value, were calculated and are shown in Figure 2. NMe-8

failed to see correlations between hydrophobicity and antimicrobial/hemolytic activity in these peptides. Thus, we believed the conformational change may be more important in affecting the antimicrobial activity of the NMe-GS analogues.

NMR study

To determine how methylation affected the backbone conformation of GS, we studied the conformations of GS, NMe-5, NMe-10, and NMe-11 using NMR analysis.^[16] 1H NMR experiments

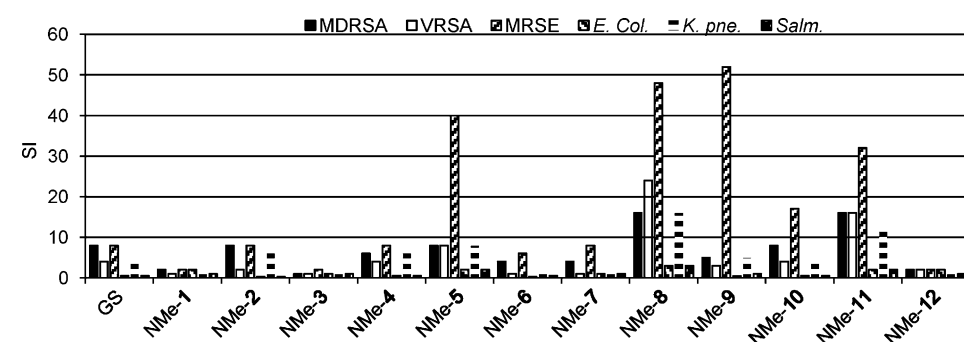


Figure 2. Selectivity index (SI) and methylated gramicidin S. $SI = HC_{50}/MIC_{90}$. *S. aureus* ATCC-BAA-44 (MDRSA), vancomycin-resistant *S. aureus* (VRSA), methicillin-resistant *S. epidermidis* (VRSE), *E. coli* k-12 (*E. coli*), *K. pneumoniae* (*K. pne.*), *Salmonella* (*Salm.*).

and NMe-11 exhibited significantly increased SI values against the entire panel of Gram-positive and -negative bacteria tested in this work. Other methylated analogues generally showed similar SI values to the one for GS, except for NMe-5 and NMe-9, whose SI values against MRSE remarkably increased. Because NMe-8, NMe-11, and NMe-5 all have a $Leu^5 \rightarrow MeLeu^5$ replacement, leading to a disruption of the internal hydrogen bonding between $Leu^5 N^H \cdots O=CVal^3$, methylation of internal hydrogen bond-forming Leu is most likely responsible for the improved selectivity for bacteria cells over human erythrocytes.

Antimicrobial and hemolytic activities of peptides are reported to link to the hydrophobicity—higher hydrophobicity of AMP was correlated with stronger antimicrobial and hemolytic activity.^[15] To determine whether hydrophobicity affected antimicrobial and hemolytic activity of the NMe-GS analogues, we compared reversed-phase HPLC retention time (t_R) with MIC_{90} and HC_{50} values separately for each analogue (Table 1), but

failed to see correlations between hydrophobicity and antimicrobial/hemolytic activity in these peptides. Thus, we believed the conformational change may be more important in affecting the antimicrobial activity of the NMe-GS analogues.

The increased $^3J_{NH-CH}$ value suggests NMe-10 has slightly distorted β -turn regions. Variable-temperature 1H NMR experiments showed the temperature shift coefficients ($\Delta\delta/\Delta T$) of the N^H s of Orn, Leu, and Val in NMe-10 decreased compared with those in GS (Table 2). The temperature shift coefficient of Leu N^H in NMe-10 decreased most significantly to -4.3 ppb K^{-1} , which is close to the indicator value of -4.5 ppb K^{-1} that separates hydrogen-bonded and nonhydrogen-bonded protons,^[17] indicating Leu N^H formed much weaker internal hydrogen bond in NMe-10 than in GS. Taken together, these data suggest that NMe-10 has a distorted β -turn and β -sheet conformation compared with GS. These results support our hypothesis that substitution of Pro with MeAla decreases structural rigidity.

NMe-5 and NMe-11 were generated by replacing $Leu^5 \rightarrow MeLeu^5$ in GS and in NMe-10, respectively. Both of them lost the C2 symmetry and differentiated nine amide protons. NMe-5 and NMe-11 had parallel $^3J_{NH-CH}$ values for the corresponding residues, suggesting these two analogues had comparable backbone conformation. The $^3J_{NH-CH}$ values of N^H s in NMe-5

Table 2. Amide proton chemical shifts δ [ppm], coupling constants $^3J_{NH-CH}$ [Hz], and temperature shift coefficients $\Delta\delta/\Delta T$ [ppb K^{-1}]. ^[a]							
Compd	δ , $^3J_{NH-CH}$ ($\Delta\delta/\Delta T$)		δ , $^3J_{NH-CH}$ ($\Delta\delta/\Delta T$)		δ , $^3J_{NH-CH}$ ($\Delta\delta/\Delta T$)		δ , $^3J_{NH-CH}$ ($\Delta\delta/\Delta T$)
	D-Phe ^{1,6}		Orn ^{4,9}		Leu ^{5,10}		Val ^{3,8}
GS	9.03, 3.2, (−7.8)		8.64, 9.2, (−5.3)		8.31, 8.8, (−2.9)		7.21, 9.6, (−1.9)
NMe-10	9.20, 2.8, (−8.0)		8.59, 9.2, (−6.1)		8.17, 9.2, (−4.3)		7.20, 9.6, (−2.6)
	D-Phe ¹	D-Phe ⁶	Orn ⁴	Orn ⁹	Leu ¹⁰	Val ³	Val ⁸
NMe-5	8.92, − ^[b] (−13.1)	7.70, 7.2, (−8.1)	8.75, 9.2, (−4.3)	8.23, 9.6, (−3.9)	8.04, 8.8, (−2.5)	6.92, 8.8, (−1.9)	7.22, 9.2, (−3.2)
NMe-11	9.21, − ^[b] (−8.5)	8.08, 6.8, (−9.6)	8.70, 9.6, (−4.0)	8.29, 8.8, (−4.0)	8.04, 9.2, (−2.8)	6.57, 8.4, (−1.4)	7.20, 9.2, (−0.3)
NMe-8	8.92, − ^[b] (−10.6)	8.26, 6.0, (−10.7)	8.32, 7.2, (−4.7)	8.73, 9.6, (−3.6)	8.16, 9.2, (−3.0)	6.59, 8.4, (−0.7)	7.21, 9.2, (−3.0)

[a] NMR experiments were performed in $[D_6]DMSO$. Chemical shifts and $^3J_{NH-CH}$ values were measured at 305 K. [b] Broad singlet.

and NMe-11 were comparable to the values in GS and NMe-10 for the corresponding residues except for D-Phe, which changed tremendously from ~3 Hz in GS/NMe-10 to ~7 Hz for D-Phe⁶, and singlet for D-Phe¹ in NMe-5/NMe-10. These substantial changes of $^3J_{\text{NH-CH}}$ values indicated the significant backbone conformational changes at the β -turn regions. Since the only difference between NMe-5 versus GS and NMe-11 versus NMe-10 is the methylation at Leu⁵, we therefore concluded methylation at Leu⁵ caused the conformational change in the β -turn region in NMe-5 and NMe-11. The temperature shift coefficients of amide N^Hs in NMe-5 and NMe-11 also exhibited a comparable pattern in that Leu¹⁰, Val⁸ and Val³ are in the range of -0.3 – -3.2 ppbK⁻¹, indicating these three N^Hs are internal hydrogen-bonded; D-Phe¹, D-Phe⁶, Orn⁴, and Orn⁹ are in the range of -3.9 to -13.1 ppbK⁻¹, suggesting these protons are solvent-exposed in both analogues. But the temperature shift coefficients of Val⁸ in NMe-11 dramatically increased to -0.3 ppbK⁻¹ compared with those of NMe-10 (-2.6), NMe-5 (-3.2), and GS (-1.9), suggesting intramolecular hydrogen bonding between Val⁸ N^H...C=O MeLeu⁵ was significantly strengthened.

NMe-8 is a dimethylated (MeAla², MeLeu⁵)-GS analogue, which kept MeLeu⁵, but differed from NMe-5 in MeAla²→Pro² and from NMe-11 in Pro⁷→MeAla⁷. The major sequence difference between NMe-8 and NMe-5/NMe-11 are Pro↔MeAla alternates at residue 2 or residue 7. ¹H NMR analysis showed that NMe-8 was similar to NMe-5 and NMe-11 in $^3J_{\text{NH-CH}}$ values, the $^3J_{\text{NH-CH}}$ value of D-Phe⁶ increased to 6 Hz, and D-Phe¹ was a singlet, suggesting significant conformational changes at β -turn regions. The temperature shift coefficients of N^Hs of NMe-8 were also similar to those of NMe-5 and NMe-11—showing N^Hs of Leu¹⁰, Val⁸ and Val³ were hydrogen-bonded, and N^Hs of D-Phe¹, D-Phe⁶, Orn⁴, and Orn⁹ were solvent-exposed. The temperature shift coefficient of Val³ significantly increased to -0.7 ppbK⁻¹, suggesting N^H of Val³ was involved in strong internal hydrogen bonding.

Conformation of the NMe-GS analogues in aqueous solution

To examine the methylation effects on conformation of NMe-GS analogues, circular dichroism (CD) spectroscopy was recorded for each analogue in an aqueous solution (see figure S5A for monomethylated NMe-GS analogues and figure S5B for di- and trimethylated NMe-GS analogues). The CD spectra for GS and the 12 NMe-GS analogues differed in shape and intensity. GS, NMe-4 (MeAla²), and NMe-10 (MeAla², MeAla⁷) presented similar CD spectra, with a negative minimum at 207 nm and a shoulder at 217 nm for a combination of type II β -turn and pleated β -sheet as reported elsewhere.^[10a,18] These data showed that the overall conformation of GS did not change when MeAla was replaced with Pro. The ratio of ellipticity of $\theta_{207}:\theta_{217}$ for GS, NMe-4, and NMe-10 is 1.04, 1.04, and 1.00, respectively. The slightly decreased ratio of $\theta_{207}:\theta_{217}$ suggested NMe-10 presented a disturbed β -turn and β -sheet conformation compared with GS in aqueous solution. All the other NMe-GS analogues showed major conformational changes, because their ellipticities were substantially changed. The CD

spectrum of NMe-2 exhibited a broad negative minimum at 207–213 nm, and NMe-3 shifted the negative minimum to 202 nm. The CD spectra of the rest of the analogues show minimum ellipticity at 217 nm and a shoulder at 207 nm, with the ellipticity ratio of $\theta_{207}:\theta_{217}$ ranging from 0.76 to 0.93. The significant decrease of ellipticity in the 200–210 nm range suggested the disruption of the β -turn part and reflected the conformational change by N-methylation. These conformational changes detected by CD spectra were correlated with the results from our NMR study. However, we have not observed the difference or trend between methylation of internal hydrogen-bonded and externally exposed amides by CD analysis. The conformational change of these analogues presented in CD spectra may also result from the formation of *cis*-peptide bond that was facilitated by methylation.^[19]

Molecular dynamics (MD) simulations

To determine how N-methylations affected the conformational properties of these analogues, we selected three with the best SI values (NMe-5, NMe-8, and NMe-11) and one (NMe-4) whose SI value was comparable to that of GS. The effects on the shapes of the rings were investigated by computing backbone radii of gyration (R_g ; see figure S1B). It is evident that the R_g value of NMe-8 and NMe-11 were larger compared with GS, NMe-4 and NMe-5. Noteworthy, NMe-5, NMe-8 and NMe-11 show lower hemolytic properties. Therefore, a scalar property such as R_g may not convey the whole picture. Thus, to identify specific overall backbone properties, the trajectories were clustered using a backbone root-mean-square deviation (RMSD) cut-off of 0.5 Å to define similar conformations using 8000 frames because of size limitations in generating the square matrix for clustering (see figure S2 for the backbone structures of the centroids from the top five clusters of each trajectory and their fractional contribution to the total population). Although the shapes of the rings and their populations reflected the values of the radius of gyration, similar atoms of the most populated clusters of GS and NMe-4 share the same prolate and oblate, and are more slender (see figure S2A and S2B). Although the R_g value of NMe-5 is comparable with that of GS, its dimensions are different (see figure S2E), tending to have a wider oblate. NMe-8 and NMe-11 share the same prolate as GS, but their oblates tend to be broader, similar to NMe-5, presumably because they are more flexible due to the absence of one (NMe-8) or two (NMe-11) Pro couple with the disruption of backbone interactions by N-methylation of Leu⁵.

GS has been described as an amphiphilic cyclic peptide, with a polar side comprising the Orn residues, and a lipophilic surface formed by the Val and Leu residues (Figure 1). Given that changes in the backbone conformation may affect the presentation of side chains, we investigated the effects of these analogues on side chain presentation (Figure 3). The side chains of the polar Orn residues are shown in Figure 3a, whereas those of the nonpolar residues are portrayed in Figures 3b,c for the five most populated clusters of each peptide.

The Orn side chains were oriented predominantly below a transverse plane of the view in Figure 3a for GS and all the

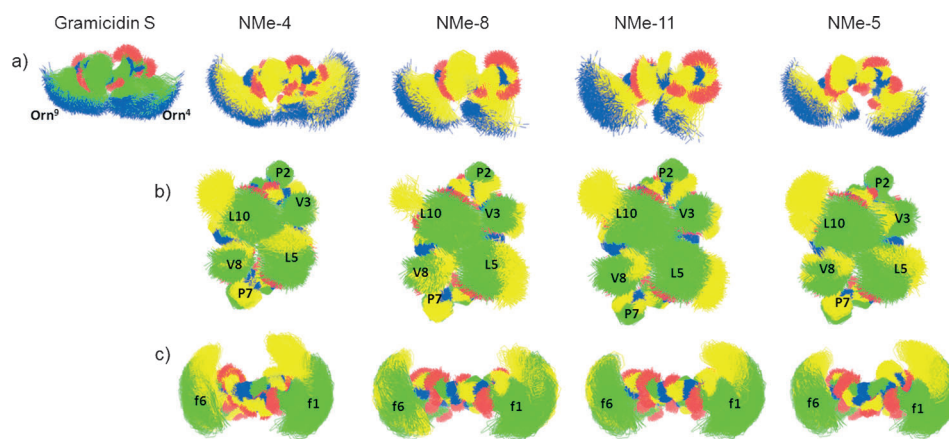


Figure 3. Side chain dispositions of GS and N-methylated analogues. a) Display of the Orn side chain. The Orn residues are shown in blue. The foremost residue in a) is P2. b) Display of hydrophobic side chains of L-amino acids. c) Display of hydrophobic side chains of D-Phe. The backbone carbon atoms of GS and each N-methylated analogue are overlapped and shown in green and yellow in a) and b), respectively. The images were generated using PyMOL (version 1.5).

peptides. However, there was a relative increase in the presence of Orn side chains along the transverse plane in the methylated analogues. These differences will invariably change the polar surface of the analogues when compared with that of GS. Interestingly, for NMe-8 and NMe-11, Orn⁴ was oriented towards a sagittal plane, whereas its orientation in NMe-4 was similar to GS. A close inspection of each individual cluster revealed that in the second most populated cluster of NMe-5, Orn⁹ was exclusively distributed close to the sagittal plane. This may have some bearing with the observed hemolytic properties of NMe-5, NMe-8, and NMe-11.

The Val and Leu residues were oriented above the transverse plane in GS, whereas this configuration was disrupted in the analogues (Figure 3b). Leu¹⁰ was displaced towards the transverse plane in all the analogues. We saw no association between the selectivity indices of these peptides with their hydrophobic group orientations.

While it may be expected that the MeAla² analogue (NMe-4) will affect the backbone conformations of local residues such as Leu¹⁰ and D-Phe¹, N-methylation of Leu⁵ affected the conformational properties of the distal Leu¹⁰ (NMe-5; Figure 3b) and D-Phe¹ (NMe-8; Figure 3c). In Figure 3c, the effect of the MeAla² substitution on the spatial display of D-Phe¹ is evident. When the MeLeu⁵ substitution was performed on NMe-4 to generate NMe-8, the side chain distribution of D-Phe¹ reverted to that observed in GS. It should be noted that NMe-8 exhibited similar space distributions of the D-Phe side chains with reference to those of GS, but possessed significantly reduced hemolytic activity. Taken together, the differences between the orientations of the Orn residues and the absence of a trend in the display of the hydrophobic groups in the low and high hemolytic peptides, suggested that the overall consequence of presentation of the Orn groups may be important for optimizing hemolytic properties.

Conclusions

Gramicidin S (GS) has all the structural elements required for β -sheet antimicrobial peptides (AMPs)—the β -turn and the anti-parallel β -strand. Methylation of its internal hydrogen-bonded amide at β -strand region terminated the specific hydrogen bonding, thereby affecting the subtle balance on backbone conformation, side chain orientation, and amphiphilicity of GS. This in turn decreased the hemolytic activity of the N-methylated products. Antimicrobial activity and hemolytic effect further dissociated when residues were methylated at both β -

strand and β -turn regions. The results provide insight into modification of other β -sheet antimicrobial peptides to improve their selectivity between bacterial cell and host cell, and impact the development of β -sheet antimicrobial peptides to therapeutic agents for clinical use.

Experimental Section

Chemistry

Synthesis: All N-methylated gramicidin S (NMe-GS) analogues were prepared by solid-phase peptide synthesis using mercaptomethyl-phenyl polystyrene resin (100 mg each, Sigma-Aldrich, loading $\sim 2.0 \text{ mmol S}^{-1} \text{ g}^{-1}$) as support. Parallel solid-phase synthesis of peptide α -thioesters were carried out using the “teabag” approach.^[20] The first amino acid, Boc-Leu-OH (5 equiv), was coupled on the resin by using benzotriazol-1-yl-oxytriethylphosphonium hexafluorophosphate (PyBOP; 5 equiv) and diisopropylethylamine (DIEA; 7.5 equiv) in *N,N*-dimethylformamide (DMF; 10 mL) overnight. Stepwise peptide synthesis was carried out using a standard diisopropylcarbodiimide (DIC)/*N*-hydroxybenzotriazole (HOBt) coupling protocol using Boc chemistry with the exception of the N-methylated amino acids and the following amino acids, which were coupled using PyBOP/DIEA activation for 2 h. After peptide chain elongation, the resin-bound peptide was treated with anhyd HF for 2 h at 0 °C. Following evaporation of anhyd HF with a gaseous nitrogen stream and washing of the resin-bound peptide with CH_2Cl_2 , the cyclic products was released by cyclization/cleavage in 10% v/v DIEA in DMF. All crude products were purified by HPLC. The LC-MS profile for each NMe-GS analogue is shown in the Supporting Information (figure S4).

NMR: All NMR spectra were recorded on a Bruker Avance III 400 high performance digital NMR spectrometer. All spectra were obtained at a concentration of 10 mM in $[\text{D}_6]\text{DMSO}$.

Circular dichroism (CD): All CD spectra were recorded on a JASCO 810 spectropolarimeter at 25 °C using a cell with 0.1 cm path length. The spectra were acquired in a wavelength range of 190–250 nm at 1 nm bandwidth using four accumulations and

200 nm min⁻¹ scanning speed. All spectra were obtained using 0.1–0.2 mM concentrations in H₂O.

Molecular dynamics (MD) simulations: The starting conformation of GS was extracted from its crystal structure complex with savinase (PDBID: 1SVN) resolved at 1.5 Å. The analogues were generated by substituting each residue of GS with the corresponding residue of the methylated analogue. The cyclic peptides were immersed in a box of TIP3P water molecules. A distance of 15 Å separated the peptides from the edges of the box. The equilibration and production stages were performed as described previously,^[21] however, production lasted 85 ns. Of note, the CHARMM parameter sets employed included CMAP terms derived for D-amino acids.^[22] NAMD v2.7b1 was employed to perform the simulations.^[23] Snapshots were collected every picosecond for post-processing. Equilibration of the MD simulations was ascertained by monitoring backbone root mean-squared deviations (RMSDs) over the course of the simulations (S1A). The RMSDs showed that the backbone cyclic systems were no longer sampling new conformers. The first 5 ns of the trajectories were discarded as additional equilibration because of fluctuations in the backbone of GS observed during this time.

Biological analysis

Antimicrobial activity: A total of three Gram-positive and three Gram-negative bacterial strains were used, including multidrug-resistant (MDR) bacterial strains: *Staphylococcus aureus* ATCC BAA-44, *Staphylococcus aureus* Mu50 (VRSA) ATCC 700699, *Staphylococcus epidermidis* (MRSE) ATCC 27626, *Escherichia coli* K-12 ATCC 29181, *Klebsiella pneumoniae* K6 ATCC 700603, and *Salmonella*. Determination of the antibacterial activity of the synthetic GS and NMe-GS analogues was performed in sterile 96-well flat-bottomed polystyrene plates by the standard microdilution broth method based on the Clinical and Laboratory Standards Institute (CLSI) protocol.^[14] Tests were performed using Müller–Hinton broth (MHB) without dilution. Controls on each plate were media without bacteria, bacterial inoculum without antimicrobials added, and bacterial inoculum containing methicillin or vancomycin. Concentrations of synthetic GS and NMe-GS analogues 1–12, as well as control antibiotics, were in the range 1–128 mg mL⁻¹. All samples were loaded in duplicate, and the average OD value was taken for calculating minimum inhibitory concentration (MIC) values. Each sample was tested twice. Stock solutions of synthesized analogues 1–12 were prepared in H₂O. Plates were loaded with 90 µL bacterial suspension (with initial OD₆₀₀ of 0.001) of the tested microorganism, and 10 µL aliquots of twofold serial dilutions of the synthetic GS and the NMe-GS analogues 1–12 or control antibiotics. Plates were then incubated at 37 °C overnight with gentle shaking. Inhibition of bacterial growth was determined by measuring OD₆₀₀; a decrease in OD₆₀₀ indicates inhibition of bacterial growth.

Hemolytic effect: Human red blood cells (hRBCs) were diluted with phosphate-buffered saline (PBS) to 0.56%. The synthetic GS and GS-NMe analogues 1–12 were dissolved in H₂O. hRBCs (90 µL) were placed into each well of the clear, flat-bottom 96-well plate, followed by the addition of analogue solution (10 µL to final peptide concentrations of 1–128 µg mL⁻¹). Assays were performed in triplicate, and each experiment was repeated twice. Hemolysis was monitored by measuring the absorbance of the released hemoglobin at 405 nm. 100% hemolysis was obtained by adding Triton X-100 aqueous solution (10 µL) to the above-prepared hRBC suspension at a final concentration of 0.5% (v/v). The minimum concentration of GS and NMe-GS analogues that required to cause 50%

hemolysis is reported as HC₅₀, where the absorbance from water (10 µL) containing no compound was used as 0% hemolysis. Plates were incubated for 1 h at 37 °C. PBS (100 µL) was added to each well, and the plates were centrifuged (10 min, 1000 g). Supernatants (100 µL) were transferred into a new plate, and absorbance at 405 nm was measured.

Abbreviations

AMP, antimicrobial peptide; Boc, *tert*-butoxycarbonyl; CD, circular dichroism; DIC, diisopropylcarbodiimide; DIEA, diisopropylethylamine; DMF, *N,N*-dimethylformamide; GS, gramicidin S; HOBt, *N*-hydroxybenzotriazole; hRBC, human red blood cells; MDR, multidrug-resistant; MIC, minimum inhibitory concentration; NMe-GS, N-methylated GS; PyBOP, benzotriazol-1-yl-oxy-tripyrrolidinophosphonium hexafluorophosphate; RMSD, root-mean-square deviation; SI, selectivity index; TFA, trifluoroacetic acid.

Acknowledgements

We acknowledge support of this work from the State of Florida (USA), Executive Office of the Governor's Development of Economic Opportunity.

Keywords: antimicrobial activity and selectivity • conformation • drug discovery • molecular modeling • peptide methylation

- [1] K. Kawano, T. Yoneya, T. Miyata, K. Yoshikawa, F. Tokunaga, Y. Terada, S. Iwanaga, *J. Biol. Chem.* **1990**, *265*, 15365–15367.
- [2] V. N. Kokryakov, S. S. Harwig, W. A. Panyutich, A. A. Shevchenko, G. M. Aleshina, O. V. Shamova, H. A. Korneva, R. I. Lehrer, *FEBS Lett.* **1993**, *327*, 231–236.
- [3] T. V. Ovchinnikova, G. M. Aleshina, S. V. Balandin, A. D. Krasnodemb-skaya, M. L. Markelov, E. I. Frolova, Y. F. Lenova, A. A. Tagaev, E. G. Krasnodemb-sky, V. N. Kokryakov, *FEBS Lett.* **2004**, *577*, 209–214.
- [4] P. M. Hwang, N. Zhou, X. Shan, C. H. Arrowsmith, H. J. Vogel, *Biochemistry* **1998**, *37*, 4288–4298.
- [5] S. U. Patel, R. Osborn, S. Rees, J. M. Thornton, *Biochemistry* **1998**, *37*, 983–990.
- [6] P. I. Silva, Jr., S. Daffre, P. Bulet, *J. Biol. Chem.* **2000**, *275*, 33464–33470.
- [7] M. Trabi, H. J. Schirra, D. J. Craik, *Biochemistry* **2001**, *40*, 4211–4221.
- [8] a) T. Mogi, H. Ui, K. Shiomi, S. Ōmura, K. Kita, *FEBS Lett.* **2008**, *582*, 2299–2302; b) T. Mogi, Y. Murase, M. Mori, K. Shiomi, S. Ōmura, M. P. Paragagama, K. Kita, *J. Biochem.* **2009**, *146*, 491–499.
- [9] a) G. M. Grotenbreg, E. Spalburg, A. J. de Neeling, G. A. van der Marel, H. S. Overkleef, J. H. van Boom, M. Overhand, *Bioorg. Med. Chem.* **2003**, *11*, 2835–2841; b) A. W. Tuin, D. K. Palachanis, A. Buizert, G. M. Grotenbreg, E. Spalburg, A. J. de Neeling, R. H. Mars-Groenendijk, D. Noort, G. A. van der Marel, H. S. Overkleef, M. Overhand, *Eur. J. Org. Chem.* **2009**, 4231–4241.
- [10] a) C. Solanas, B. G. de La Torre, M. Fernández-Reyes, C. M. Santiveri, M. A. Jiménez, L. Rivas, A. I. Jiménez, D. Andreu, C. Catiuela, *J. Med. Chem.* **2009**, *52*, 664–674; b) C. Solanas, B. G. de La Torre, M. Fernández-Reyes, C. M. Santiveri, M. A. Jiménez, L. Rivas, A. I. Jiménez, D. Andreu, C. Catiuela, *J. Med. Chem.* **2010**, *53*, 4119–4129.
- [11] E. J. Prenner, M. Kiricsi, M. Jelokhani-Niaraki, R. N. A. H. Lewis, R. S. Hodges, R. N. McElhaney, *J. Biol. Chem.* **2005**, *280*, 2002–2011.
- [12] B. Laufer, J. Chatterjee, A. O. Frank, H. Kessler, *J. Pept. Sci.* **2009**, *15*, 141–146.

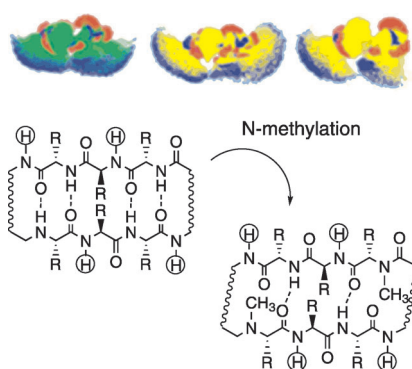
- [13] a) Y. Li, Y. Yu, M. Giulianotti, R. A. Houghten, *J. Comb. Chem.* **2008**, *10*, 613–616; b) J. A. Camarero, A. Adeva, T. W. Muir, *Lett. Pept. Sci.* **2000**, *7*, 17–21.
- [14] N. Bionda, M. Stawikowshi, R. Stawikowska, M. Cudic, F. López-Vallejo, D. Treitl, J. Medina-Franco, P. Cudic, *ChemMedChem* **2012**, *7*, 871–882.
- [15] a) T. Wieprecht, M. Dathe, M. Beyermann, E. Krause, W. L. Maloy, D. L. MacDonald, M. Bienert, *Biochemistry* **1997**, *36*, 6124–6132; b) Y. Chen, M. T. Guarnieri, A. I. Vasil, M. L. Vasil, C. T. Mant, R. S. Hodges, *Antimicrob. Agents Chemother.* **2007**, *51*, 1398–1406.
- [16] a) E. M. Krauss, S. I. Chan, *J. Am. Chem. Soc.* **1982**, *104*, 6953–6961; b) K. Yamada, S.-s. Shinoda, H. Oku, K. Komagoe, T. Katsu, R. Katakai, *J. Med. Chem.* **2006**, *49*, 7592–7595.
- [17] N. J. Baxter, M. P. Williamson, *J. Biomol. NMR* **1997**, *9*, 359–369.
- [18] a) M. Kawai, H. Yamamura, R. Tanaka, H. Umemoto, C. Ohmizo, S. Higuchi, T. Katsu, *J. Pept. Res.* **2005**, *65*, 98–104; b) M. Jelokhani-Niaraki, R. S. Hodges, J. E. Meissner, U. E. Hassenstein, *Biophys. J.* **2008**, *95*, 3306–3321.
- [19] C. McInnes, L. H. Kondejewski, R. S. Hodges, B. D. Sykes, *J. Biol. Chem.* **2000**, *275*, 14287–14292.
- [20] R. A. Houghten, *Proc. Natl. Acad. Sci. USA* **1985**, *82*, 5131–5135.
- [21] A. B. Yongye, Y. Li, M. A. Giulianotti, Y. Yu, R. A. Houghten, K. Martínez-Mayorga, *J. Comput.-Aided Mol. Des.* **2009**, *23*, 677–689.
- [22] E. R. Turpin, J. D. Hirst, *Chem. Phys. Lett.* **2012**, *543*, 142–147.
- [23] J. C. Phillips, R. Braun, W. Wang, J. Gumbart, E. Tajkhorshid, E. Villa, C. Chipot, R. D. Skeel, L. Kalé, K. Schulten, *J. Comput. Chem.* **2005**, *26*, 1781–1802.

Received: May 21, 2013

Published online on ■ ■ ■ ■, 0000

FULL PAPERS

Out of order! Disruption of the internal hydrogen bond(s) of β -sheet antimicrobial peptides by N-methylation could improve their selectivity for microbial cells over erythrocytes. We investigated a model β -sheet antimicrobial peptide, gramicidin S, for the N-methylation effects on antimicrobial and hemolytic activities. ^1H NMR and circular dichroism spectroscopy results show that N-methylation of the internal hydrogen bond-forming amide affected the conformation, backbone shape, and side chain orientation.



Y. Li,* N. Bionda, A. Yongye, P. Geer, M. Stawikowski, P. Cudic, K. Martinez, R. A. Houghten*

■■ – ■■

Dissociation of Antimicrobial and Hemolytic Activities of Gramicidin S through N-Methylation Modification

